THE LANCET
Public Health

Supplementary appendix

This appendix formed part of the original submission and has been peer reviewed. We post it as supplied by the authors.

Supplement to: Leung K, Wu JT, Leung GM. Effects of adjusting public health, travel, and social measures during the roll-out of COVID-19 vaccination: a modelling study. *Lancet Public Health* 2021; published online August 10. http://dx.doi.org/10.1016/S2468-2667(21)00167-5.

Supplementary information

Table of Contents

The age-structured Susceptible-Infectious-Removed model

We used our previous age-structured SIR model to simulate the transmission of SARS-CoV-2 [1]:

$$\frac{dS_{n,a}(t)}{dt} = -S_{n,a}(t)\pi_a(t)$$

$$\frac{dS_{v,a}(t)}{dt} = -(1-\sigma_m)S_{v,a}(t)\pi_a(t)$$

$$\frac{\partial I_{n,a}(t,\tau)}{\partial t} + \frac{\partial I_{n,a}(t,\tau)}{\partial \tau} = -f_{GT}(\tau)I_{n,a}(t,\tau)$$

$$\frac{\partial I_{v,a}(t,\tau)}{\partial t} + \frac{\partial I_{v,a}(t,\tau)}{\partial \tau} = -f_{GT}(\tau)I_{v,a}(t,\tau)$$

$$I_{n,a}(t,0) = S_{n,a}(t)\pi_a(t)$$

$$I_{v,a}(t,0) = (1-\sigma_m)S_{v,a}(t)\pi_a(t)$$

$$\frac{dR_{n,a}(t)}{dt} = \int_0^t f_{GT}(\tau)I_{n,a}(t,\tau)d\tau$$

$$\frac{dR_{v,a}(t)}{dt} = \int_0^t f_{GT}(\tau)I_{v,a}(t,\tau)d\tau$$

$$N_{n,a} = S_{n,a}(t) + \int_0^t I_{n,a}(t,\tau)d\tau + R_{n,a}(t)$$

$$N_{v,a} = S_{v,a}(t) + \int_0^t I_{v,a}(t,\tau)d\tau + R_{v,a}(t)$$

$$\pi_a(t) = \sum_{b=1}^{m}\int_0^t \frac{\beta_{ab}(t)}{N_b}\Big(I_{n,b}(t,\tau) + (1-\sigma_t)I_{v,b}(t,\tau)\Big)\,d\tau$$

where

- σ_m was the vaccine efficacy in reducing susceptibility to SARS-CoV-2 infection.
- σ_t was the vaccine efficacy in reducing infectivity of SARS-CoV-2.
- m was the number of age groups in the population.
- $c_{ab}(t)$ was the average rate at which an individual in age group *a* made infectious contacts with age group *b* at time *t*.
- $\beta_{ab}(t) = \alpha_a\gamma_b c_{ab}(t)$ in which α_a was the relative susceptibility of age group *a* and γ_b was the relative infectiousness of age group *b*.
- The next generation matrix (NGM) for this SIR model was

$$NGM(t) = T_{GT}\begin{bmatrix} \beta_{11}(t) & \cdots & \beta_{1m}(t) \\ \vdots & \ddots & \vdots \\ \beta_{m1}(t) & \cdots & \beta_{mm}(t) \end{bmatrix}$$

where T_{GT} was the mean generation time. The effective reproductive number $R_e(t)$ in the absence of vaccination or immunity was the spectral radius of this matrix.

- $S_{n,a}(t)$ and $R_{n,a}(t)$ were the number of susceptible and removed individuals among those who were not vaccinated in age group a at time *t*.
- $S_{v,a}(t)$ and $R_{v,a}(t)$ were the number of susceptible and removed individuals among those who were vaccinated in age group a at time *t*.
- $I_{n,a}(t,\tau)$ was the number of infectious individuals among those who were not vaccinated in age group *a* at time *t* who were infected at time $t-\tau$.
- $I_{v,a}(t,\tau)$ was the number of infectious individuals among those who were vaccinated in age group *a* at time *t* who were infected at time $t-\tau$.
- $N_{n,a}$ was the total number of people who were not vaccinated in age group a.
- $N_{v,a}$ was the total number of people who were vaccinated in age group a.
- $\pi_a(t)$ was the force of infection on age group a at time t.
- f_{GT} was the pdf of the generation time.

The incidence rate of infections and symptom onsets in age group a at time t were calculated as follows:

$$A_{a,infection}(t) = \left(S_{n,a}(t) + (1-\sigma_m)S_{v,a}(t)\right)\pi_a(t)$$

$$A_{a,onset}(t) = p_{a,onset}\int_0^t A_{a,infection}(u)\, f_{incubation}(t-u)du$$

where $p_{a,onset}$ was the probability of developing symptoms among infections in age group a and $f_{incubation}$ was the probability density function (pdf) of the incubation period. Similarly, the incidence rate of hospitalizations and deaths were calculated as follows:

$$A_{a,hospitalization}(t)$$
$$= p_{a,hospitalization}\int_0^t \left(S_{n,a}(t) + (1-\sigma_m)(1-\sigma_s)S_{v,a}(t)\right)\pi_a(t)\, f_{hospitalization}(t-u)du$$

$$A_{a,death}(t)$$
$$= p_{a,death}\int_0^t \left(S_{n,a}(t) + (1-\sigma_m)(1-\sigma_s)S_{v,a}(t)\right)\pi_a(t)\, f_{death}(t-u)du$$

where $p_{a,hospitalization}$ and $p_{a,death}$ were the probability of hospitalizations and deaths among infections in age group a, $f_{hospitalization}$ was the pdf of the time between infection and hospitalization, and f_{death} was the pdf of the time between infection and death.

Quantifying the reduction in infectiousness of an imported infection

We assume that once infected, unvaccinated and vaccinated individuals have the same infectiousness profile. We also assume that the temporal distribution of infectiousness is the same for symptomatic and asymptomatic infections (but they may have different magnitude of infectiousness). Let $g(\cdot)$ be the pdf of incubation period and $h(\cdot)$ be the temporal distribution of infectiousness relative to the time of symptom onset. We assume that $g(\cdot)$ is lognormal with the mean of 5.22 (95% CI 4.1-7.0) days [2] and $h(\cdot)$ is the same inferred infectiousness profile by days after symptom onset (i.e., -10 – 8 days) in Figure 2C as in our previous study [3]. The temporal distribution of infectiousness t days after infection is obtained by convoluting the two distributions (Figure S7):

$$f(t) = \int_0^t g(u)h(t-u)du$$

Let $F(t) = \int_0^t f(u)\,du$, which is the cumulative temporal distribution of infectiousness *t* days after infection. Given that we are only concerned about the temporal distribution but not the absolute magnitude of infectiousness, we set $F(\infty) = 1$ without loss of generality.

The effect of testing and quarantine on reducing the expected force of infection (FOI) exerted by infected travellers on the destination

Let $p_{PCR}(t)$ be the sensitivity of RT-PCR test for an individual who has been infected for *t* days (Figure S7). We estimate $p_{PCR}(t)$ based on the data from Kucirka et al [4]. If an infected individual is test-negative on day *t* and then tested again on day *t* + *d*, we assume that the correlation between the sensitivity of the two tests is a function of *d* as shown in Figure S8.

Suppose an infected traveller is infected *d* days before arrival and will be quarantined for q days if test-negative upon arrival (the FOI posed by him/her on the destination is highest if he/she is infected immediately before arrival because he/she will be test-negative upon arrival). The expected cumulative infectiousness that this traveller poses on the destination is

$$G(d,q,1) = \left(1 - p_{pcr}(d)\right)(F(\infty) - F(d+q)) = \left(1 - p_{pcr}(d)\right)(1 - F(d+q))$$

if there is no test upon quarantine release and

$$G(d,q,2) = G(d,q,1)(1 - p_{pcr}(d+q))$$

if he/she is tested again upon quarantine release. Note that these are an upper-bounds because the calculations ignore the possibility that the infected traveller could be detected and isolated during quarantine (e.g., due to overt symptoms).

Determining the eligibility for inbound travel from different origins

We first consider a single origin. We assume that vaccinated and unvaccinated individuals are subject to the same FOI at the origin. Let π_u and π_v be the prevalence of infection among unvaccinated and vaccinated travellers arriving from the origin. π_u and π_v can be estimated from either (i) the observed number of infections detected among unvaccinated and vaccinated inbound travellers arriving from the origin; or (ii) the incidence statistics (adjusted for under-ascertainment) and vaccine coverage at the origin [5]. For the latter, if the incidence statistics are not stratified by vaccination status, then π_u and π_v can be crudely estimated from the overall prevalence (π) and vaccine coverage (v) at the origin by assuming that $\pi_v = (1-\sigma_m)\,\pi_u$ and

$$\pi = (1-v)\pi_u + v(1-\sigma_m)\pi_u$$

where *v* is the vaccine coverage at the origin.

Let n_u and n_v be the number of unvaccinated and vaccinated inbound travellers on a given day. The expected FOI from these travellers is

$$FOI_{import} < G(0,q,s)(n_u\pi_u + n_v(1-\sigma_m)\pi_u)$$

Note that $G(0,0,0) = F(\infty) = 1$ and hence FOI_{import} can also be interpreted as the expected number of undetected infections among inbound travellers (as in Figure 3 in the main text). To avoid underestimating FOI_{import}, we ignore the effect of vaccine efficacy in reducing infectivity. If only vaccinated travellers are allowed for entry, the expected FOI from these travellers reduces to

$$FOI_{import} < G(0,q,s)n_v(1-\sigma_m)\pi_u$$

On the other hand, the FOI exerted by the local cases is

$$FOI_{local} = i_D F(\infty) = i_D \approx \pi_D N_D/T$$

where i_D is the daily number of infections at the destination, π_D is the prevalence of infections at the destination, N_D is the population size of the destination and T is the duration of infection.

We propose that measures for preventing infection importation from the origin (i.e., quarantine, testing and ceilings on n_u and n_v) should be maintained to ensure that FOI_{import} is small compared to FOI_{local}. For example, $FOI_{import} < \varepsilon FOI_{local}$ where ε is a risk threshold set by the destination on the origin (say $\varepsilon = 0.01$). This condition would be satisfied if

$$G(0,q,s)(n_u\pi_u + n_v(1-\sigma_m)\pi_u) < \varepsilon FOI_{local}$$

If COVID-19 has been eliminated at the destination for a prolonged period, εFOI_{local} can be replaced with the daily number of infections that the destination can confidently contain without substantial socioeconomic disruption.

In the general case where there are multiple origins (denoted by the subscript *i* in what follows), the above criterion is naturally generalized to $\sum_i FOI_{import,i} < FOI_{local} \sum_i \varepsilon_i$ which would hold if

$$\sum_i G(0,q_i,s_i)\left(n_{u,i}\pi_{u,i} + n_{v,i}(1-\sigma_m)\pi_{u,i}\right) < FOI_{local} \sum_i \varepsilon_i$$

Under this formulation, the quarantine duration, testing requirement, ceilings on inbound volume and risk threshold for each origin would be judiciously determined by the destination when prescribing the eligibility criteria for each origin (e.g., with respect to their social, economic and political importance to the destination).

Determining the trigger of the circuit breaker

We now describe the algorithm for monitoring whether the actual number of detected infections among travellers arriving from a given origin conforms with the above-mentioned eligibility criteria. If the detected number of infected travellers is higher than expected, then a circuit breaker will be triggered to suspend travellers from that origin and the corresponding eligibility criteria will be updated in light of that data.

Let m_i be the daily average detected number of infected travellers arriving at the destination. If the PCR test sensitivity for detecting infections is p_{sens} = 62% (i.e., within the range of 60-65% estimated from Hong Kong data), the maximum expected daily FOI exerted by infected travellers on the destination is $G(0,q_i,s_i)m_i/p_{sens}$. To keep the maximum expected FOI from these inbound travellers below a given threshold γ_i (which might be slightly higher than $\varepsilon_i FOI_{local}$ from the previous section in order to account for effects such as clustering of cases due to family or group travel and stochasticity), we require $G(0,q_i,s_i)m_i/p_{sens} < \gamma_i$. This is equivalent to triggering the circuit breaker if the daily average number of detected infections among arriving inbound travellers exceeds $\frac{p_{sens}\gamma_i}{G(0,q_i,s_i)}$.

In the illustrative example shown in Figure 4 in the main text, we assume $\gamma_i = 0.8$ (i.e., 80% of the expected total FOI from a typical infection) and all inbound travellers are quarantined for 4 days and tested twice. In this case, the circuit breaker would be triggered when the daily average number of detected infections among arriving inbound travellers exceeds $\frac{p_{sens}\gamma_i}{G(0,4,2)} \approx 5$.

We can further include the effects of stochasticity when determining the trigger for the circuit breaker. For example, assuming that the number of infected travellers follows a Poisson distribution, the circuit breaker could be triggered if the number of infections detected among arriving travellers exceeds a prespecified percentile of $Poisson\left(\frac{p_{sens}\gamma_i}{G(0,q_i,s_i)}\right)$ (e.g. lower percentiles correspond to more stringent criteria).

Supplementary Tables

Table S1. Model parameters

Parameter	Description, assumption and source	Value
R_e	Effective reproductive number in the absence of vaccination, considering the emergence of VOCs (assumed)	1.0 – 9.0
T_{GT}	Mean generation time [6]	Figure 1 and S1: 5.4 days Figure S2: 4.4, 5.4, or 6.4 days
f_{GT}	Probability density function of generation time [6]	Figure 1 and S1: Gamma (4, 1.35) Figure S2: Gamma (4, 1.1), Gamma (4, 1.35), or Gamma (4, 1.6)
σ_m	Vaccine efficacy in reducing susceptibility (assumed)	0.5, 0.6, 0.7, or 0.8
σ_t	Vaccine efficacy in reducing infectivity (assumed)	0.3, 0.4, or 0.5
σ_s	Vaccine efficacy in reducing symptomatic diseases and hospitalizations (assumed)	0.8, 0.9, or 0.95
$p_{a,death}$	Age-specific infection fatality risk [7,8]	Figure 1, S1 and S2: Age 0-9: 0.00161% Age 10-19: 0.00695% Age 20-29: 0.0309% Age 30-39: 0.0844% Age 40-49: 0.161% Age 50-59: 0.595% Age 60-69: 1.93% Age 70-79: 4.28% Age ≥ 80: 7.80% or Figure S2: Age 0-34: 0.003% Age 35-54: 0.076% Age 55-69: 0.59% Age 70-84: 6.0% Age ≥ 85: 23%
$p_{a,hospitalization}$	Age-specific infection hospitalization risk [7]	Figure 1, S1 and S2: Assumed to be 20 times of the age-specific infection fatality risk Figure S2: Age 0-9: 0.00161% Age 10-19: 0.0408% Age 20-29: 1.04% Age 30-39: 3.43% Age 40-49: 4.25% Age 50-59: 8.16% Age 60-69: 11.8% Age 70-79: 16.6% Age ≥ 80: 18.4% or

		Assumed to be 5, 10, 20 times of the age-specific infection fatality risk
$f_{incubation}$	Probability density function of incubation period [2]	Lognormal distribution Mean: 5.22 days SD: 3.9 days
$f_{hospitalization}$	Probability density function of the time between infection and hospitalization (assumed)	Gamma distribution Mean: 8 days SD: 3.6 days
f_{death}	Probability density function of the time between infection and death; estimated from $f_{incubation}$ and the probability density function of the time between onset and death (Mean 18.8 days and SD 8.46 days) from Verity et al [7];	Gamma distribution Mean: 23.0 days SD: 9.9 days
H_{max}	The maximum number of COVID-19 hospitalizations that the local health system could take care of per day (assuming it is similar to the daily number of COVID-19 hospitalizations admitted in the UK in early Jan 2021 [9]; On 1 Jan 2021, the number of hospital admissions in the UK was 3,371; The maximum daily number of hospital admissions in the UK since the emergence of COVID-19 was 4,574 on 12 Jan 2021)	0.005% of the total population

Supplementary Figures

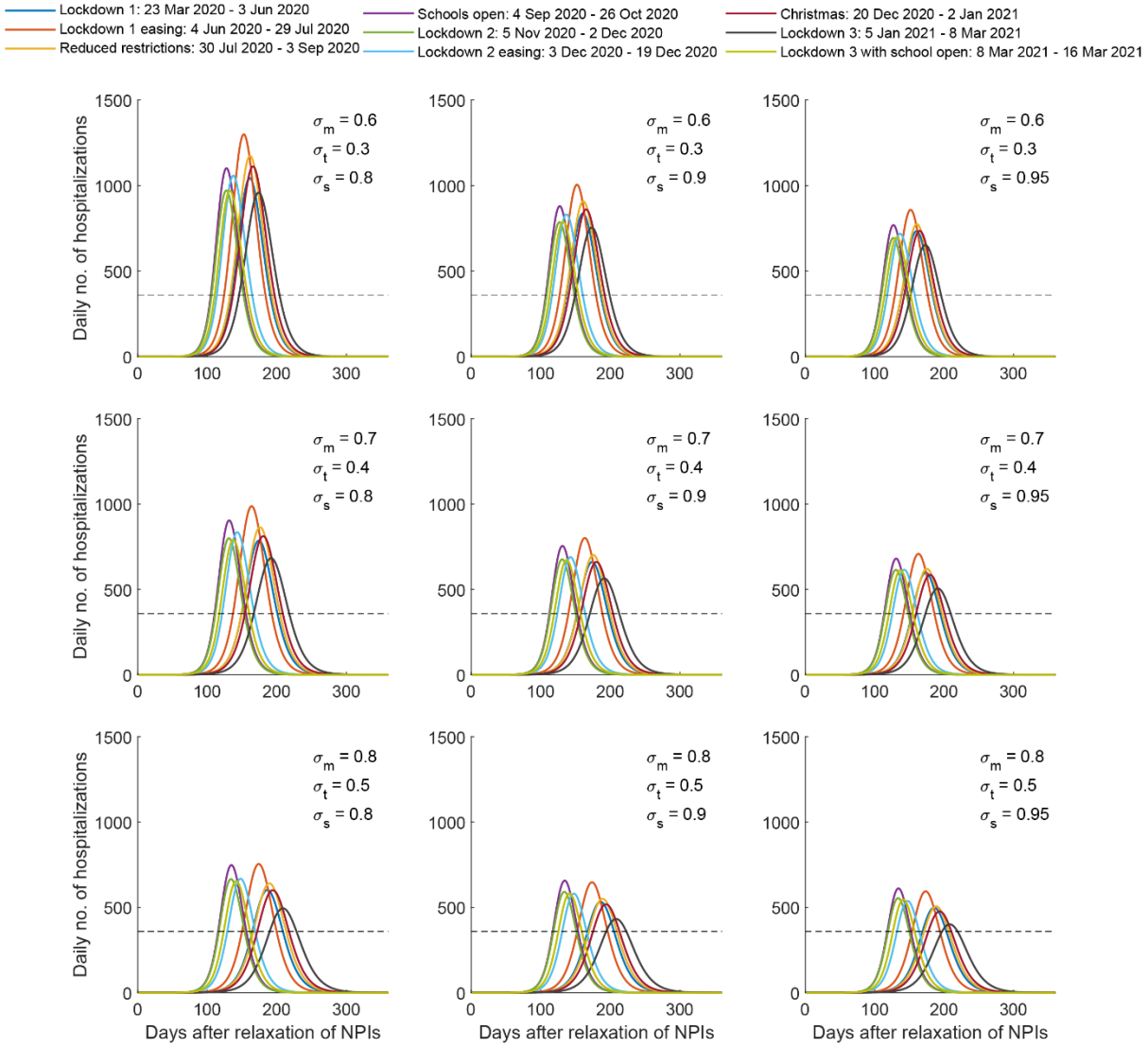

Figure S1. The effects of different contact patterns on the outcomes of PHSM relaxations in Hong Kong. The contact matrices were obtained from different periods in the CoMix contact survey in the UK (https://cmmid.github.io/topics/covid19/comix-reports.html). We estimated daily hospitalizations in Hong Kong following relaxation of PHSMs after all individuals aged 50 or above have been vaccinated, assuming $R_e = 1.3$. Other parameters were the same as that in the scenario of $R_e = 1.3$ in Figure 1. When vaccine efficacies are high (e.g., $\sigma_m = 0.8$, $\sigma_t = 0.5$ and $\sigma_s = 0.95$), the peak of hospitalizations is delayed and the peak size of hospitalizations is also reduced, if we assume contact pattens from the periods when the most stringent PHSMs were implemented in the UK (e.g., during Lockdown 1 between 23 Mar and 3 Jun 2020, and Christmas and Lockdown 3 between 20 Dec 2020 and 8 Mar 2021).

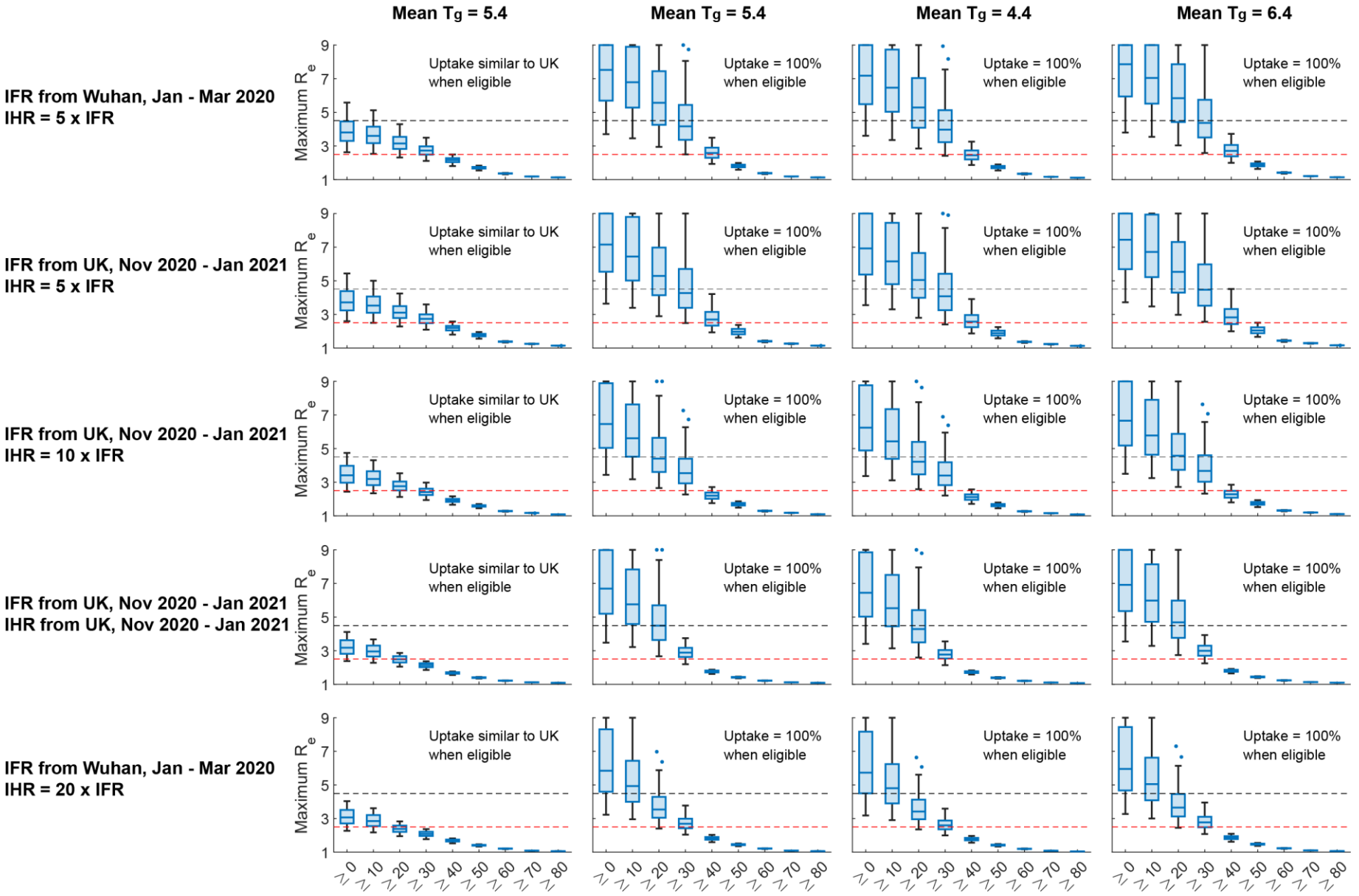
Mean Tg = 5.4
Mean Tg = 5.4
Mean Tg = 4.4
Mean Tg = 6.4
IFR from Wuhan, Jan - Mar 2020
IHR = 5 x IFR
IFR from UK, Nov 2020 - Jan 2021
IHR = 5 x IFR
IFR from UK, Nov 2020 - Jan 2021
IHR = 10 x IFR
IFR from UK, Nov 2020 - Jan 2021
IHR from UK, Nov 2020 - Jan 2021
IFR from Wuhan, Jan - Mar 2020
IHR = 20 x IFR
Maximum Re
Uptake similar to UK when eligible
Uptake = 100% when eligible
≥ 0
≥ 10
≥ 20
≥ 30
≥ 40
≥ 50
≥ 60
≥ 70
≥ 80

Figure S2. Boxplots of the maximum R_e that prevents COVID-19 hospitalizations from overloading the health system in Hong Kong following the relaxation of PHSMs across different vaccination scenarios and assumptions regarding infection fatality risk (IFR), infection hospitalization risk (IHR) and mean generation time. R_e is the effective reproductive number after relaxation of PHSMs in the absence of vaccination. Vaccines are prioritized for individuals aged *X* or above (x-axis). In the first column, the age-specific vaccine uptake is similar to that of the UK on 6 Jun 2021, and the uptake for those younger than 30 is similar to that of the 30-39 age group when they are eligible for vaccination. In the second to fourth column, vaccine uptake is 100% among all eligible individuals. In each panel, we assume the vaccine efficacy is $\sigma_m \in (0.5, 0.6, 0.7, 0.8)$ in reducing the susceptibility to SARS-CoV-2 infection, $\sigma_t \in (0.3, 0.4, 0.5)$ in reducing SARS-CoV-2 infectivity and $\sigma_s \in (0.8, 0.9, 0.95)$ in reducing symptomatic COVID-19 diseases (i.e., 36 combinations in total). The maximum capacity of the health system (in terms of daily hospital admissions) is 0.005% of the population size. The red dashed line shows $R_e = 2.5$ and black dashed line shows $R_e = 4.5$.

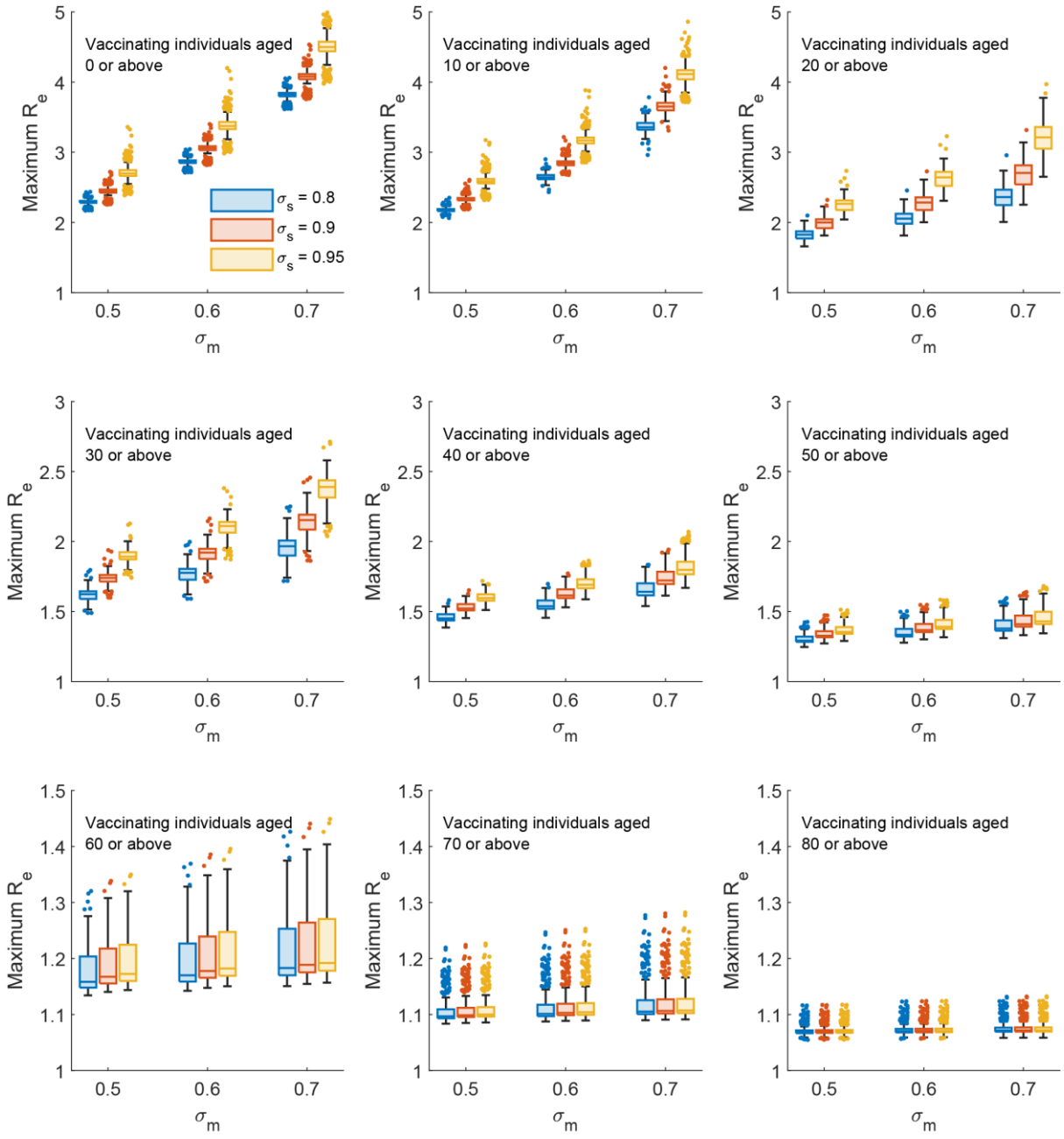

Figure S3. Boxplots of the maximum R_e that maintains the daily number of hospitalizations below the threshold of the healthcare capacity following the relaxation of PHSMs under different vaccination coverages. We assume vaccines are allocated from oldest to youngest age groups, and all individuals who are eligible for vaccination are vaccinated before any PHSMs are relaxed (100% uptake). Conservatively we assume the vaccine efficacy is $\sigma_m \in (0.5,0.6,0.7)$ in reducing the susceptibility to SARS-CoV-2 infection, $\sigma_t = 0$ in reducing SARS-CoV-2 infectivity and $\sigma_s \in (0.8,0.9,0.95)$ in reducing symptomatic COVID-19 diseases. The threshold of the healthcare capacity is assumed to be 0.005% of the total population of 27 countries and 277 sub-national administrative regions (of 8 countries) in which the simulations are performed. Country-level age demographics and contact patterns of the 35 countries are from Mistry et al [10]. The ranges of y-axis are different for each row to increase readability.

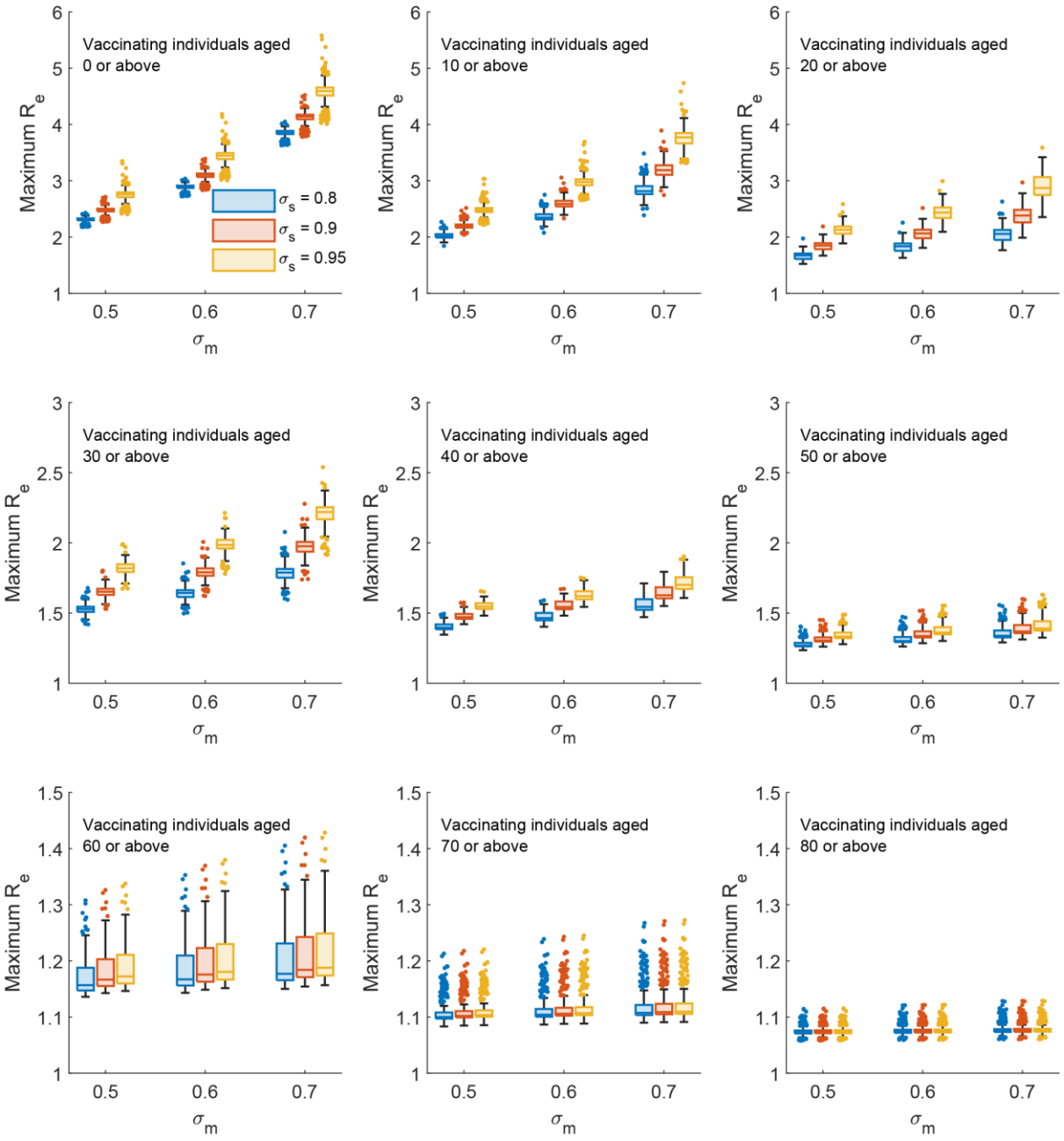

Figure S4. The maximum R_e that maintains the daily number of hospitalizations below the threshold of the healthcare capacity following the relaxation of PHSMs under different vaccination coverages. Similar to Figure S3 but assuming children and adolescents are as susceptible and infectious as adults. The ranges of y-axis are different for each row to increase readability.

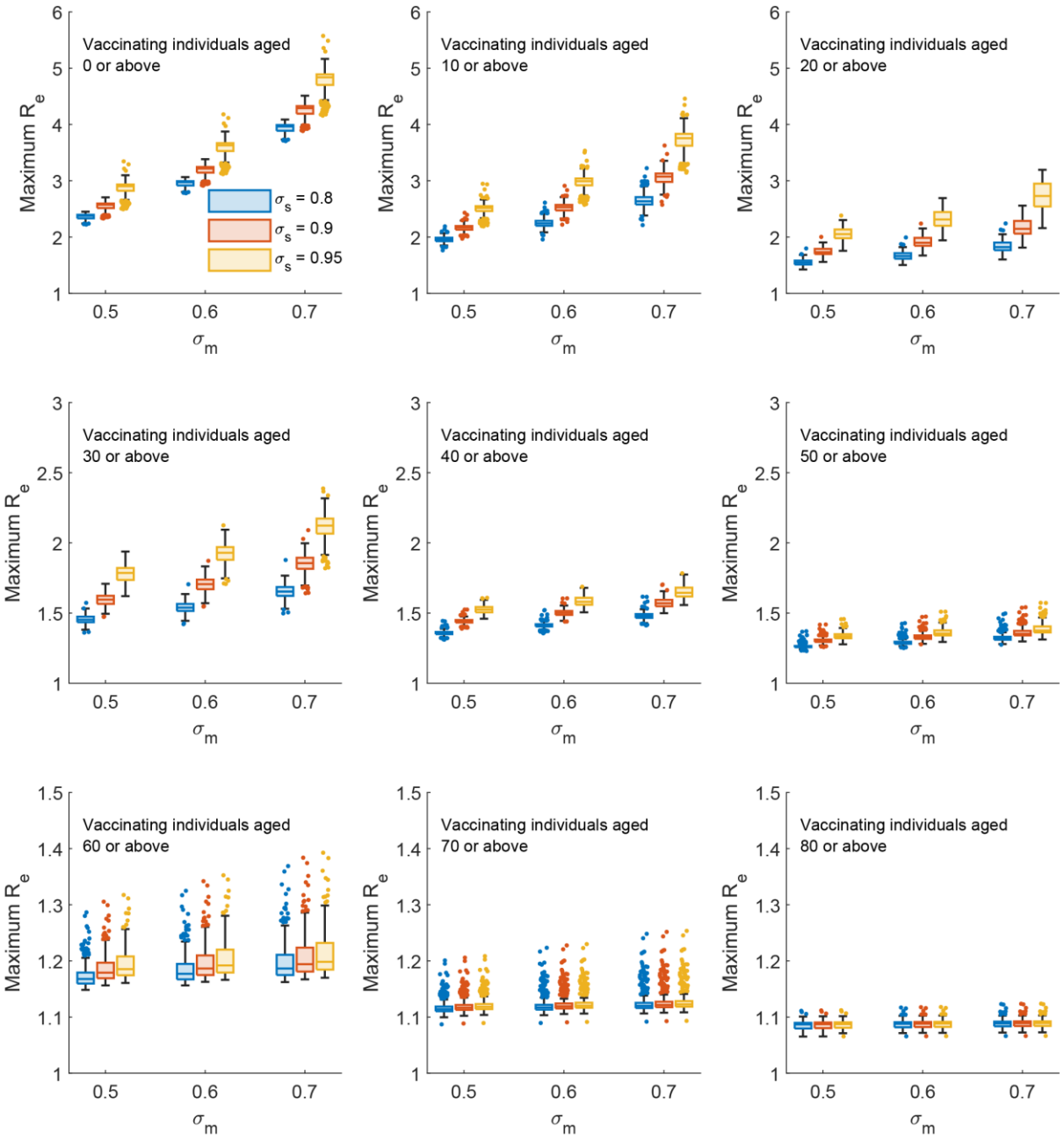

Figure S5. The maximum R_e that maintains the daily number of hospitalizations below the threshold of the healthcare capacity following the relaxation of PHSMs under different vaccination coverages. Similar to Figure S3 but assuming children and adolescents are as susceptible as adults but 50% more infectious than adults. The ranges of y-axis are different for each row to increase readability.

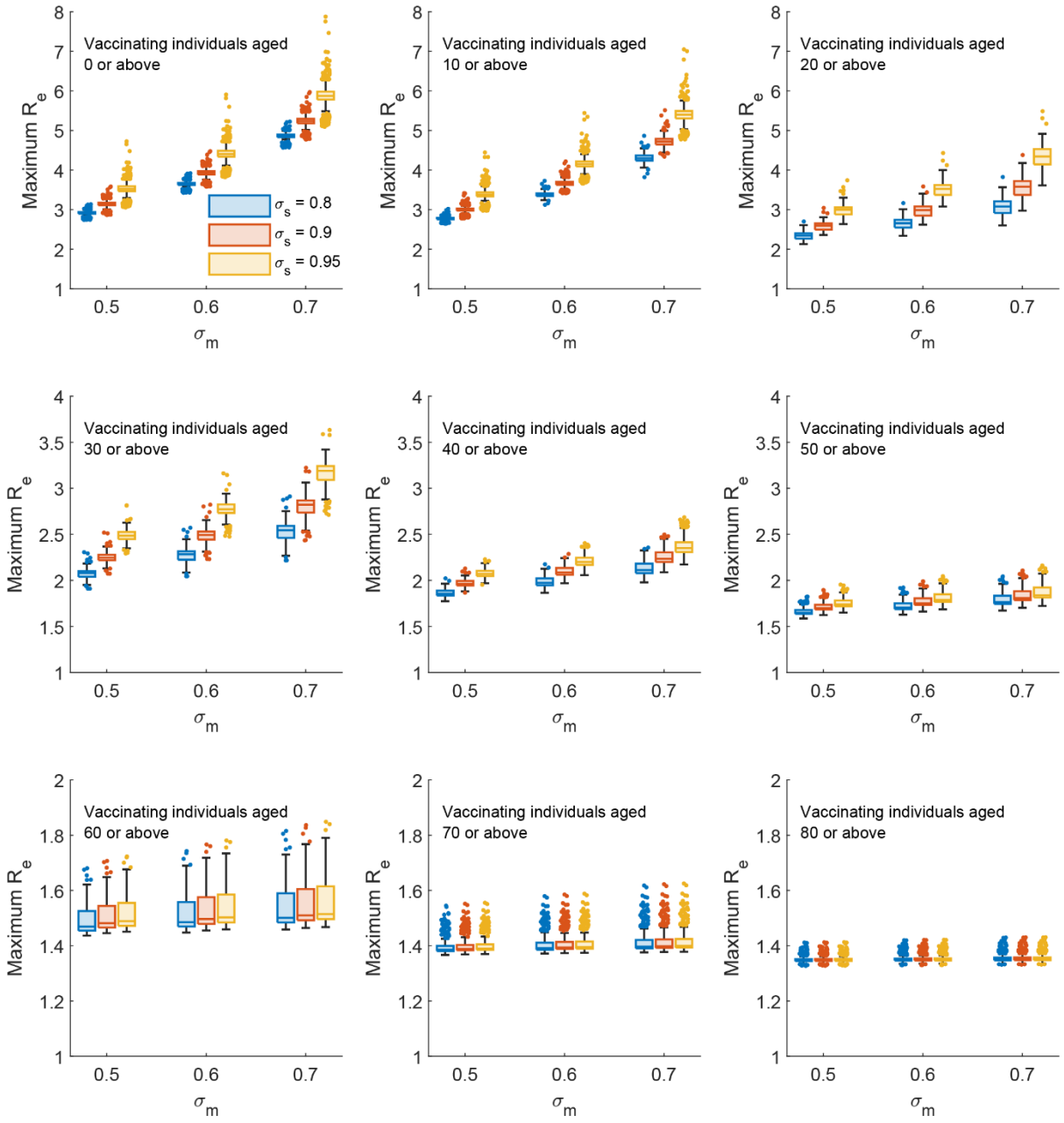

Figure S6. The maximum R_e that maintains the daily number of hospitalizations below the threshold of the healthcare capacity following the relaxation of PHSMs under different vaccination coverages. Similar to Figure S3 but assuming 20% of all age groups of the population have been infected before and immune to SARS-CoV-2 infection before vaccination. The ranges of y-axis are different for each row to increase readability.

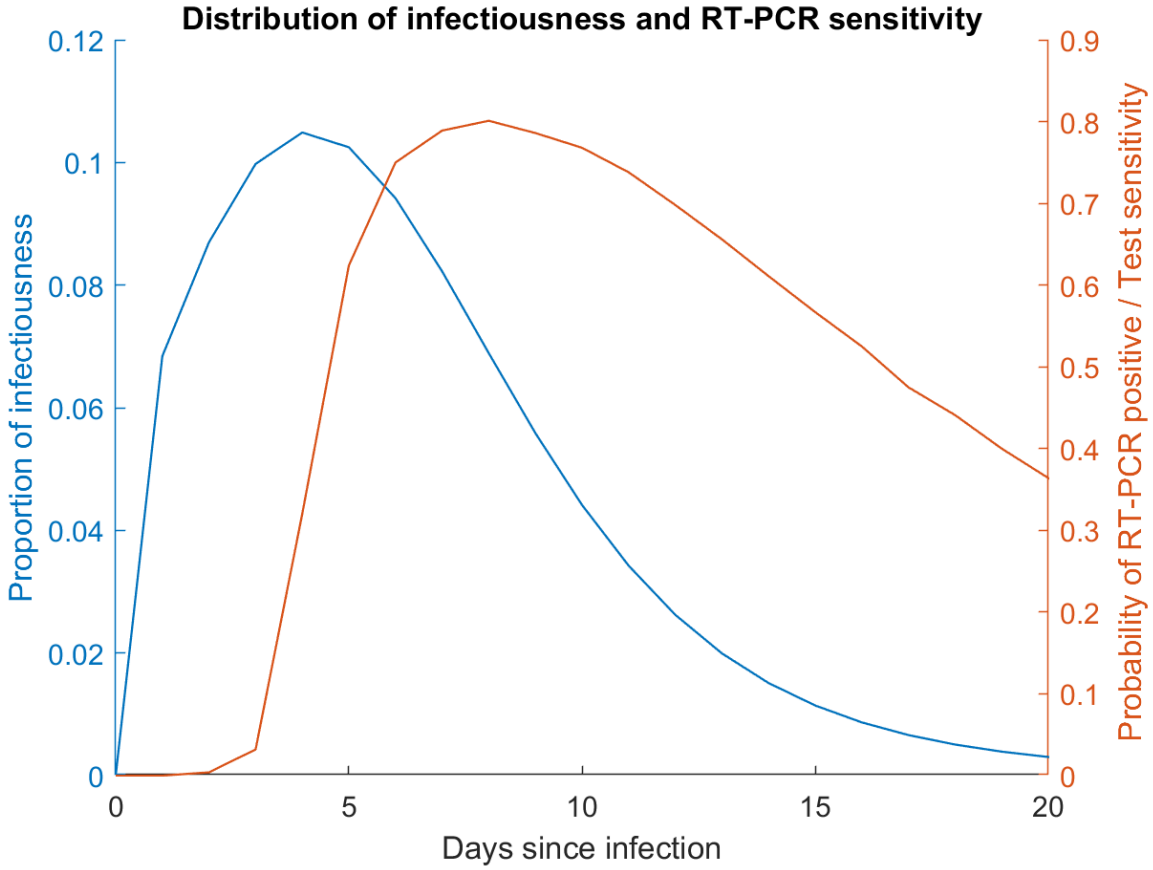

Figure S7. Distribution of infectiousness and the sensitivity of RT-PCR by days since infection. We assume the incubation period is lognormal distributed with the mean of 5.22 (95% CI 4.1-7.0) days [2]. We assume the distribution of infectiousness by days after symptom onset is the same as in our previous study [3]. The distribution of infectiousness by days since infection (blue line) is obtained by integrating the two distributions. The sensitivity of RT-PCR by days since infection (orange line) is adapted from Figure 2 of Kucirka LM and Lauer SA et al [4].

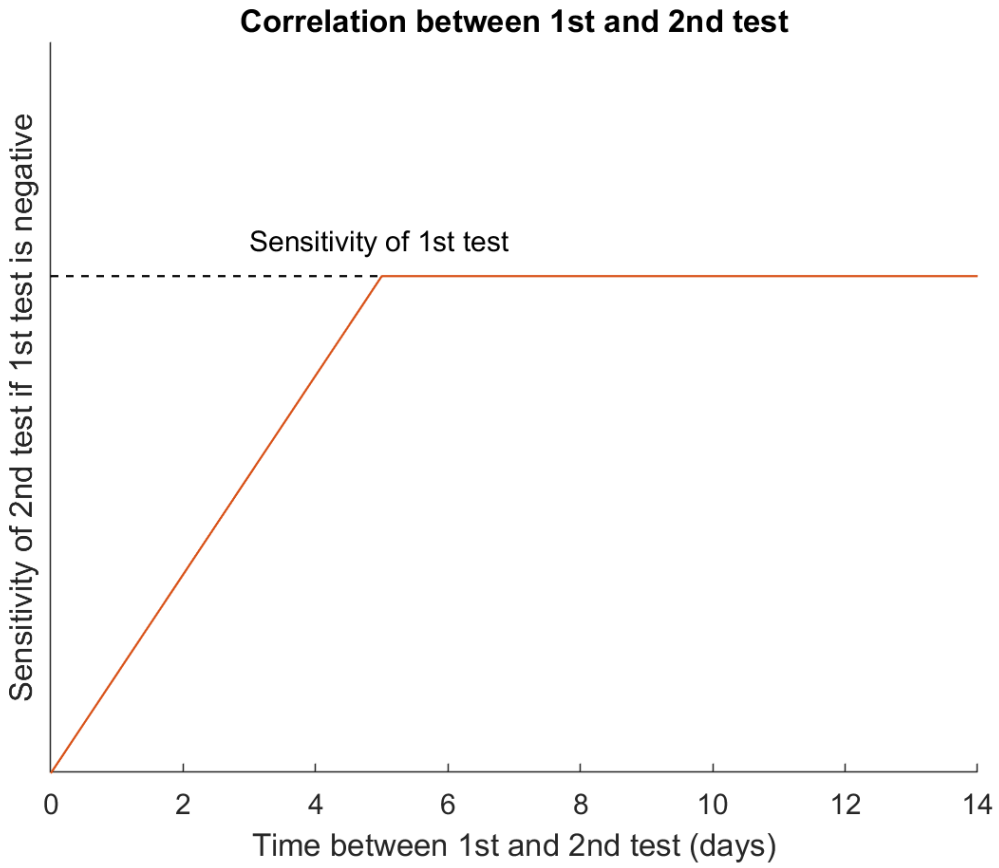

Figure S8. Assumption about the sensitivity of the second test if the first test is negative. If the first test is negative, the sensitivity of the second test is dependent on: 1) the viral load of the individual during different time periods of the infection, and 2) the characteristics of the test (e.g., RT-PCR or alternative tests). Therefore, we assume that the sensitivity of the second test follows a linear relationship above. The sensitivity of the first and second test are independent if the time between the two tests is ≥ 5 days. The correlation between the sensitivity of the two tests is assumed to avoid overestimating the effects of testing, especially when the time interval between the two tests is very short. In Hong Kong, as of 15 Jun 2021, all inbound travellers from places of origins with moderate to high COVID-19 prevalence in Group A1, A2, B and C are required to be tested four times and quarantined for 21 days (https://www.coronavirus.gov.hk/eng/high-risk-places.html).

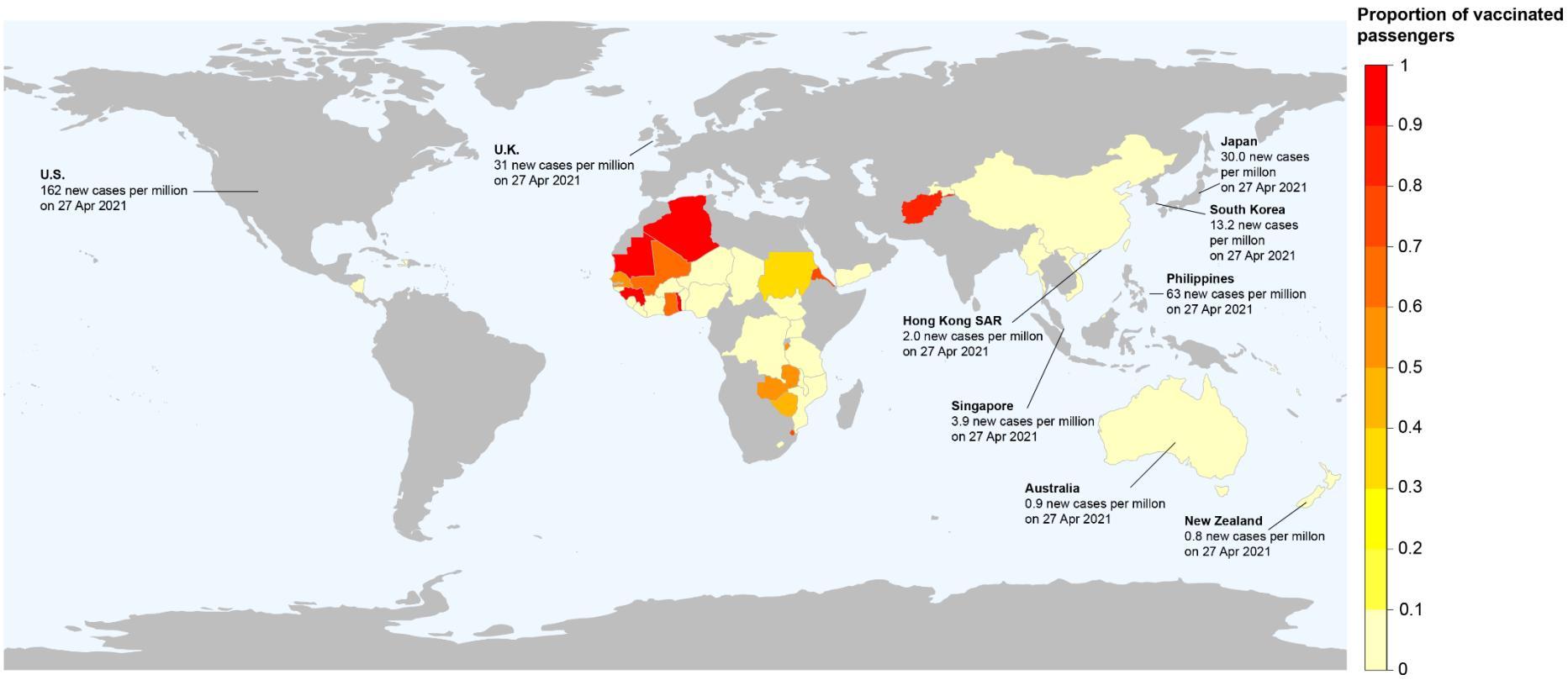

Figure S9. The minimum proportion of vaccinated passengers on a "safe" flight by country or region of origin. We assume Hong Kong is the destination with a risk tolerance level of 2.0 new local cases per million population per day (i.e., 15 new cases in a 7.45 million population). Assuming a vaccine with $\sigma_m = 60\%$ is available worldwide, the map is showing the minimum proportion of vaccinated passengers on a "safe" flight by places of origin, using the risk assessment tool described in the Supplementary Information. There are either no case data in countries and regions in grey colour or that the SARS-CoV-2 prevalence at the origin is too high such that even if all passengers are vaccinated, the prevalence among inbound passengers would still be higher than risk tolerance level.

References

1. Wu JT, Leung K, Bushman M, et al. Estimating clinical severity of COVID-19 from the transmission dynamics in Wuhan, China. *Nature Medicine* 2020.
2. Li Q, Guan X, Wu P, et al. Early Transmission Dynamics in Wuhan, China, of Novel Coronavirus–Infected Pneumonia. *New England Journal of Medicine* 2020.
3. He X, Lau EH, Wu P, et al. Temporal dynamics in viral shedding and transmissibility of COVID-19. *Nature medicine* 2020: 1-4.
4. Kucirka LM, Lauer SA, Laeyendecker O, Boon D, Lessler J. Variation in false-negative rate of reverse transcriptase polymerase chain reaction–based SARS-CoV-2 tests by time since exposure. *Annals of Internal Medicine* 2020.
5. Russell TW, Wu JT, Clifford S, Edmunds WJ, Kucharski AJ, Jit M. Effect of internationally imported cases on internal spread of COVID-19: a mathematical modelling study. *The Lancet Public Health* 2021; **6**(1): e12-e20.
6. Leung K, Wu JT, Liu D, Leung GM. First-wave COVID-19 transmissibility and severity in China outside Hubei after control measures, and second-wave scenario planning: a modelling impact assessment. *The Lancet* 2020.
7. Verity R, Okell LC, Dorigatti I, et al. Estimates of the severity of coronavirus disease 2019: a model-based analysis. *The Lancet Infectious Diseases* 2020; **20**(6): 669-77.
8. Davies NG, Jarvis CI, Edmunds WJ, Jewell NP, Diaz-Ordaz K, Keogh RH. Increased mortality in community-tested cases of SARS-CoV-2 lineage B. 1.1. 7. *Nature* 2021; **593**(7858): 270-4.
9. GOV.UK. Coronavirus (COVID-19) in the UK: Healthcare in United Kingdom. 2021. https://coronavirus.data.gov.uk/details/healthcare.
10. Mistry D, Litvinova M, Pastore y Piontti A, et al. Inferring high-resolution human mixing patterns for disease modeling. *Nature Communications* 2021; **12**(1): 323.